

EVOLUTION AND PULSATION PERIOD CHANGE IN THE LARGE MAGELLANIC CLOUD CEPHEIDS

Yu. A. Fadeyev*

*Institute of Astronomy, Russian Academy of Sciences, Pyatnitskaya ul. 48, Moscow, 109017
Russia*

Received June 3, 2013

Abstract — Theoretical estimates of the pulsation period change rates in LMC Cepheids are obtained from consistent calculation of stellar evolution and nonlinear stellar pulsation for stars with initial chemical composition $X = 0.7$, $Z = 0.008$, initial masses $5M_{\odot} \leq M_{\text{ZAMS}} \leq 9M_{\odot}$ and pulsation periods ranged from 2.2 to 29 day. The Cepheid hydrodynamical models correspond to the evolutionary stage of thermonuclear core helium burning. During evolution across the instability strip in the HR diagram the pulsation period Π of Cepheids is the quadratic function of the evolution time for the both fundamental mode and first overtone. Cepheids with initial masses $M_{\text{ZAMS}} \geq 7M_{\odot}$ pulsate in the fundamental mode and the period change rate $\dot{\Pi}$ varies nearly by a factor of two for both crossings of the instability strip. In the period – period change rate diagram the values of Π and $\dot{\Pi}$ concentrate within the strips, their slope and half-width depending on both the direction of the movement in the HR–diagram and the pulsation mode. For oscillations in the fundamental mode the half-widths of the strip are $\delta \log \dot{\Pi} = 0.35$ and $\delta \log \dot{\Pi} = 0.2$ for the first and the secon crossings of the instability strip, respectively. Results of computations are compared with observations of nearly 700 LMC Cepheids. Within existing observational uncertainties of $\dot{\Pi}$ the theoretical dependences of the period change rate on the pulsation period are in a good agreement with observations.

Keywords: *stars: variable and peculiar.*

INTRODUCTION

Periods of light variations in many δ Cep pulsating type variables (Cepheids) are known with eight significant digits (Samus et al. 2012). So high accuracy of determination of the period Π is due excellent repetition of pulsation motions and also is owing to the fact that photographic observations of Cepheids are carried out since the end of the XIX century, so that photometric measurements of some stars of this type cover as many as several thousands oscillation cycles. In such a case the long-term observations allow us to significantly correct the value of the period with the $O - C$ diagram. At the same time as early as in the thirties of the XX century the $O - C$ diagrams of some Cepheids were found to have the quadratic

*E-mail: fadeyev@inasan.ru

term indicating the secular period change (Kukarkin and Florja 1932). Interest in such a property grew after works by Hofmeister et al. (1964) and Iben (1966) where the evolutionary state of Cepheids was determined and long-term period changes were thought to be due to evolutionary changes of the stellar structure during thermonuclear core helium burning (Ferne 1979; Mahmoud and Szabados 1980; Szabados 1983; Deasy and Wayman 1985).

In recent years a great deal of observational data on long-term pulsation period changes in the Large Magellanic Cloud (LMC) Cepheids was obtained in ASAS, MACHO and OGLE projects. Pietrukowicz (2001) considered data on 378 LMC Cepheids and concluded that all studied variables with periods longer 8 days show period changes. Later Poleski (2008) carried out an analysis of 655 LMC Cepheids and found that 18% of fundamental mode and 41% of first overtone pulsators have evolutionary period changes.

The estimation of the period change rate \dot{P} from observations is of great interest since it provides with the direct test of the stellar evolution theory. Unfortunately, theoretical studies of pulsation period changes in Cepheids based on consistent solution of the equations of stellar evolution and stellar pulsation have not been done yet. Pietrukowicz (2001) compared his observational data with evolutionary and pulsation models studied by Alibert et al. (1999) and Bono et al. (2000). However the pulsation period change rates \dot{P} were not evaluated in these theoretical works, so that Pietrukowicz (2001) used rough estimates from presented tabular data. Moreover, Alibert et al. (1999) in their linear analysis of pulsational instability did not take into account effects of convection. Such a simplification might be responsible for a large disagreement between theoretical models and observational estimates of \dot{P} (Pietrukowicz 2001). Poleski (2008) compared his observational data with stellar evolution theory using the approach by Turner et al. (2006) which is also based on strong simplifications.

The goal of the present work is to obtain theoretical estimates of the pulsation period change rate \dot{P} as a function of the age of the Cepheid using the consistent calculations of stellar evolution and nonlinear stellar pulsation. Initial relative mass abundances of hydrogen and elements heavier than helium correspond to the LMC chemical composition: $X = 0.7$, $Z = 0.008$. In hydrodynamical calculations of nonlinear stellar pulsations we take into account effects of turbulent convection, so that the hydrodynamical models occupy the whole interval of effective temperatures bounded in the Hertzsprung–Russel (HR) diagram by the blue and red edges of the instability strip. Methods of stellar evolution calculation and basic equations of radiation hydrodynamics and turbulent convection used for calculation of nonlinear stellar pulsation are given in our previous paper (Fadeyev 2013).

RESULTS OF COMPUTATIONS

Solution of the equations of hydrodynamics for nonlinear stellar oscillations as a function of time t was done with initial conditions taken in the form of stellar models of evolutionary sequences of stars with initial masses $5M_{\odot} \leq M_{\text{ZAMS}} \leq 9M_{\odot}$. Evolutionary tracks in the HR diagram of stars under consideration are shown in Fig. 1 where in dotted lines are shown parts of the track corresponding to the instability against radial oscillations. In the starting and in the ending track points the rate of the thermonuclear energy generation rate $\varepsilon_{\text{n,c}}$ and the rate of the gravitational energy production $\varepsilon_{\text{g,c}}$ in the stellar center are nearly the same: $\varepsilon_{\text{n,c}} \approx \varepsilon_{\text{g,c}}$. Therefore the tracks displayed in Fig. 1 represent the evolutionary stage when the only source of energy generation in the stellar center is thermonuclear helium burning.

For each evolutionary track the bounds of pulsational instability in the HR diagram were determined from hydrodynamical computations where as in our previous work (Fadeyev 2013) the kinetic energy of pulsation motions E_{K} was calculated. The part of the evolutionary track with pulsational instability was determined from condition $\eta > 0$, where $\eta = \Pi^{-1} d \ln E_{\text{Kmax}}/dt$ is the growth rate of the kinetic energy, E_{Kmax} is the maximum value of the kinetic energy reached during one pulsational cycle. The pulsation period Π was evaluated from the discrete Fourier transform of the kinetic energy E_{K} . It should be noted that the interval of time t within of which we integrate equations of hydrodynamics is comparable with the thermal scale of outer layers of the Cepheid and is much shorter in comparison with the nuclear evolution time scale. For example, in the Cepheid with initial mass $M_{\text{ZAMS}} = 7M_{\odot}$ the evolution time between the red and blue edges of the instability strip is $\sim 10^5$ years, whereas hydrodynamic computations of the instability growth with subsequent limit cycle attainment are done on the time interval of ~ 10 years.

In Fig. 2 we give the plots of the instability growth rate η versus effective temperature averaged over the pulsational cycle $\langle T_{\text{eff}} \rangle$ for four Cepheid evolutionary sequences with initial masses from $5M_{\odot}$ to $8M_{\odot}$. The evolutionary track crosses the instability strip twice in the HR diagram and therefore each evolutionary sequence is represented by two plots where the first one corresponds to the movement across the HR diagram with increasing effective temperature (dotted lines) and the second plot corresponds to the movement in the opposite direction (dash-dotted lines). In Fig. 2 we use the averaged over the cycle effective temperature $\langle T_{\text{eff}} \rangle$ as independent variable because in the hydrodynamical model the average radius of the photosphere $\langle r_{\text{ph}} \rangle$ is smaller than the radius of the photosphere of the hydrostatically equilibrium model $r_{\text{ph},0}$. For hydrodynamical models of Cepheids calculated in the present study the ratio of the photosphere radii ranges within $0.975 \leq \langle r_{\text{ph}} \rangle / r_{\text{ph},0} < 1$ and edges of the instability strip shift to the blue in the HR diagram by $30 \text{ K} < \Delta T_{\text{eff}} < 70 \text{ K}$.

The presence of two maxima in plots of η for $M_{\text{ZAMS}} \leq 6M_{\odot}$ is due to the fact that near the red edge of the instability strip radial pulsations are excited in the fundamental mode, whereas at higher effective temperatures pulsations are excited in the first overtone. Transition between oscillation modes takes place within the effective temperature range $6000 \text{ K} < \langle T_{\text{eff}} \rangle < 6100 \text{ K}$.

In Cepheids with initial mass $M_{\text{ZAMS}} = 7M_{\odot}$ evolving blueward across the instability strip radial oscillations are due to instability of the fundamental mode and transition to the first overtone takes place just near the blue edge at $\langle T_{\text{eff}} \rangle \approx 6200 \text{ K}$. During the second crossing of the instability strip radial oscillations exist in the form of the fundamental mode.

Pulsations of Cepheids with initial mass $M_{\text{ZAMS}} \geq 8M_{\odot}$ are always due to instability of the fundamental mode and the pulsation period Π gradually changes while the star moves in the HR diagram from one edge of the instability strip to another. The change of the pulsation period of the Cepheid with initial mass $M_{\text{ZAMS}} = 8M_{\odot}$ is illustrated in Fig. 3 where for the sake of convenience we set the evolution time t_{ev} to zero when the star crosses the edge of the instability strip and begins to oscillate. The plot with gradual decrease of the pulsation period corresponds to the first crossing of the instability strip and the plot with gradually increasing period corresponds to the second crossing. Hydrodynamical models with positive and negative growth rates η are shown in filled circles and opened circles, respectively. As is seen from shown plots the pulsation period Π is fitted by an algebraic polynomial $\Pi(t_{\text{ev}}) = a_0 + a_1 t_{\text{ev}} + a_2 t_{\text{ev}}^2$ for both evolutionary sequences with a good accuracy (i.e. with relative r.m.s. error less than one per cent). Polynomial approximation is shown in Fig. 3 by dotted and dash-dotted lines for the first crossing and the second crossing of the instability strip, respectively.

Expression of the pulsation period Π as a quadratic polynomial of t_{ev} was found to be a good approximation for all Cepheid models considered in the present study. The only exception is a discontinuity of the period due to transition from one pulsation mode to other. This is illustrated in Fig. 4 by the plots of the pulsation period for the Cepheid with initial mass $M_{\text{ZAMS}} = 6M_{\odot}$. However within the interval of the continuous change of Π the quadratic polynomial remains a quite good approximation.

The quadratic dependence of the pulsation period Π on the evolutionary time t_{ev} implies the linear change of $\dot{\Pi}$ which decreases during the first crossing of the instability strip and increases during the next crossing. In Cepheids pulsating in the fundamental mode within the whole instability strip the period change rate $\dot{\Pi}$ varies roughly by a factor of two. Typical values of $\dot{\Pi}$ can be found in the table where for the evolutionary sequences with initial masses $5M_{\odot} \leq M_{\text{ZAMS}} \leq 9M_{\odot}$ we give the main properties of Cepheids at the points where the evolutionary track crosses the edges of the instability strip. Each evolutionary sequence is represented by four lines where the first pair of lines corresponds to the first crossing of the

instability strip and the second pair of lines corresponds to the second crossing. In the second column of the table we give the evolution time Δt_{ev} spent by the Cepheid within instability strip. In following columns we give main parameters of the Cepheid at the edge of the instability strip (i.e. for $\eta = 0$) which were obtained by linear interpolation of model parameters of adjacent hydrodynamical models with opposite signs of the growth rate of kinetic energy. The model parameters are as follows: the stellar mass M which is less than the initial mass M_{ZAMS} due to effects of the stellar wind during the preceding evolution; the averaged over the cycle absolute bolometric luminosity L and effective temperature $\langle T_{\text{eff}} \rangle$; the pulsation period Π , the dimensionless pulsation period change rate $\dot{\Pi}$; the order of the pulsation mode k ($k = 0$ for the fundamental mode and $k = 1$ for the first overtone).

COMPARISON WITH OBSERVATIONS

The period of light variations is the only quantity which can be determined from observations of the pulsating variable star with sufficiently high precision. Therefore for comparison of the results of theoretical computations with observational data we will consider the period change rate $\dot{\Pi}$ as a function of the pulsation period Π .

In Fig. 5 the plots of the dimensionless period change rate $\dot{\Pi}$ are shown as a function of the pulsation period Π for the Cepheid models crossing blueward the instability strip. The plots are separated into two groups with Cepheids pulsating in the fundamental mode ($6.9 \text{ day} \leq \Pi \leq 28 \text{ day}$) and those pulsating in the first overtone ($2.2 \text{ day} \leq \Pi \leq 4.5 \text{ day}$). The plots locate along the dashed lines which are approximately given by following relations

$$\log(-\dot{\Pi}) = \begin{cases} -11.71 + 4.836 \log \Pi, & k = 0, \\ -9.676 + 2.562 \log \Pi, & k = 1, \end{cases} \quad (1)$$

where the period Π is expressed in days, whereas $k = 0$ and $k = 1$ correspond to the fundamental mode and to the first overtone, respectively. Due to the finite width of the instability strip the plots of evolutionary sequences shown in Fig. 5 by solid lines are confined within the bands with half-width $\delta \log \dot{\Pi} = 0.035$ for $k = 0$ and $\delta \log \dot{\Pi} \approx 0.1$ for $k = 1$.

The diagram period – period change rate for Cepheids of the second crossing of the instability strip is shown in Fig. 6. Unfortunately, reliable estimates of the period change rate for Cepheid models with initial mass $M_{\text{ZAMS}} = 5M_{\odot}$ evolving redward in the HR diagram were not obtained, so that in Fig. 6 the mean dependence of the period change rate is shown only for the fundamental mode:

$$\log \dot{\Pi} = -10.33 + 3.386 \log \Pi. \quad (2)$$

The half-width of the band in the period – period change rate diagram is $\delta \log \dot{\Pi} = 0.2$.

To compare results of our theoretical computations with observations we used observational estimates of the period Π and the period change rate $\dot{\Pi}$ from works by Pietrukowicz (2001) and Poleski (2008). Electronic tables 1 – 3 supplementing the paper by Pietrukowicz (2001) give data on 369 LMC Cepheids, whereas the period change rates were evaluated using the Harvard photographic observations obtained in time interval from 1910 to 1950. Observational data on LMC Cepheids obtained from the OGLE survey were received from the author (Poleski 2008).

The diagram period – period change rate for Cepheids crossing the instability strip blueward with negative $\dot{\Pi}$ is presented in Fig. 7a and the same diagram for Cepheids evolving redward with positive $\dot{\Pi}$ is shown in Fig. 7b. Results of observations obtained by Pietrukowicz (2001) and Poleski (2008) are shown by filled circles and open circles, respectively. Theoretical dependences obtained in the present study for Cepheid evolutionary sequences with initial masses from 5 to $9M_{\odot}$ are shown in solid lines. In general one can conclude that the theory of stellar evolution agrees with observations of Cepheids.

At the same time one should note a disagreement between observational results by Pietrukowicz (2001) and those by Poleski (2008). A possible cause of such a difference seems to be a shorter time interval used by Poleski (2008) for evaluation of the Cepheid period changes.

CONCLUSION

Results of our calculations allow us to conclude that the oscillation period Π of the Cepheid is the quadratic function of the evolution time t_{ev} and when the star crosses the instability strip the quantity $\dot{\Pi}$ changes by a factor of two. Earlier Deasy and Wayman (1985) noted the occurrence of non-constant period change in LMC Cepheids.

An interesting result of our calculations is that the dependence of the period change rate $\dot{\Pi}$ on the pulsation period Π for the fundamental mode differs from that for the first overtone. Unfortunately, at present observational confirmation of this feature seems to be impossible because of insufficiently high accuracy of observational evaluation of $\dot{\Pi}$ for the first overtone Cepheids. Significant scatter of points in Fig. 7 at short periods ($\Pi < 7$ day) is mainly due to the power law decrease of $\dot{\Pi}$ with decreasing pulsation period. Indeed, as is seen in Fig. 5 the period change rates in first overtone Cepheids are three orders of magnitude smaller in comparison with those in long period ($\Pi \approx 30$ day) Cepheids. Therefore, to reduce the error of the observational estimate of $\dot{\Pi}$ in first overtone pulsators to the value comparable with that in long period Cepheids the time interval of the $O - C$ diagram should be expanded by two orders of magnitude.

Thus, for comparison of the stellar evolution calculations with observations of most interest are fundamental mode Cepheids. Here among the important questions we should emphasize

the role of chemical composition and convective overshooting in the period – period change rate diagram. It should also be noted that the crossing time of the Cepheid instability strip by core helium burning stars with initial masses $M_{\text{ZAMS}} > 9M_{\odot}$ becomes comparable with that during the gravitational contraction of the helium core before the stage of the red supergiant. Therefore the most massive long period Cepheids with gravitationally contracting core may play perceptible role in the period – period change rate diagram.

The author thanks Radek Poleski who kindly placed the Cepheid OGLE data at his disposal. The study was supported by the Basic Research Program of the Russian Academy of Sciences “Nonstationary phenomena in the Universe”.

REFERENCES

1. Y. Alibert, I. Baraffe, P. Hauschildt, et al., *Astron.Astrophys.* **344**, 551 (1999).
2. G. Bono, F. Caputo, S. Cassisi, et al., *Astrophys.J.* **543**, 955 (2000).
3. H.P. Deasy and P.A. Wayman, *MNRAS* **212**, 395 (1985).
4. Yu.A. Fadeyev, *Pis'ma Astron. Zh.* **39**, 342 (2013) [*Astron.Lett.* **39**, 306 (2013)].
5. J.D. Fernie, *Astrophys. J.* **231**, 841 (1979).
6. E. Hofmeister, R. Kippenhahn and A. Weigert, *Zeitschrift für Astrophys.* **60**, 57 (1964).
7. I. Iben, *Astrophys.J.* **143**, 483 (1966).
8. B.W. Kukarkin and N. Florja, *Zeitschrift für Astrophys.* **4**, 247 (1932).
9. F. Mahmoud and L. Szabados, *IBVS*, N 1895, 1 (1980).
10. P. Pietrukowicz, *Acta Astron.* **51**, 247 (2001).
11. R. Poleski, *Acta Astron.* **58**, 313 (2008).
12. N.N. Samus, O.V. Durlevich, E.V. Kazarovets, et al., *General Catalogue of Variable Stars* (GCVS database, version April 2012), CDS B/gcvs (2012).
13. L. Szabados, *Astrophys. Space Sci* **96**, 185 (1983).
14. D. Turner, M. Abdel-Sabour Abdel-Latif, and L.N. Berdnikov, *PASP* **118**, 410 (2006).

Cepheid models at the edges of the instability strip

$M_{\text{ZAMS}}/M_{\odot}$	$\log \Delta t_{\text{ev}}, \text{ year}$	M/M_{\odot}	$L/L_{\odot}, 10^4$	$\langle T_{\text{eff}} \rangle, \text{ K}$	$\Pi, \text{ day}$	$\dot{\Pi}, 10^{-7}$	k
9	3.57	8.715	1.4081	5467	25.62	-70.3	0
		8.715	1.4259	6012	18.17	-39.1	0
	3.89	8.664	1.5440	5905	20.98	16.0	0
		8.664	1.5106	5458	27.59	30.5	0
8.5	3.77	8.262	1.1553	5475	22.13	-42.9	0
		8.262	1.1718	6079	15.36	-19.3	0
	4.12	8.216	1.3126	6025	17.45	9.74	0
		8.215	1.2784	5464	24.58	19.7	0
8	3.98	7.806	0.9313	5510	18.58	-23.0	0
		7.806	0.9454	6134	12.78	-10.5	0
	4.31	7.764	1.0937	6092	14.88	5.76	0
		7.763	1.0615	5459	21.68	12.6	0
7	4.88	6.871	0.5775	5548	12.95	-3.84	0
		6.869	0.5937	6303	5.70	-0.347	1
	4.73	6.831	0.7204	6255	10.31	1.72	0
		6.829	0.6963	5512	15.75	3.99	0
6	5.71	5.917	0.3436	5635	8.70	-0.295	0
		5.913	0.3716	6548	3.76	-0.0699	1
	5.31	5.889	0.4285	6444	4.46	0.219	1
		5.886	0.4129	5595	10.54	1.15	0
5	6.09	4.955	0.1874	5796	5.26	-0.0604	0
		4.952	0.2096	6808	2.31	-0.0193	1
	6.20	4.947	0.2208	6771	2.46	0.0174	1
		4.942	0.2178	5751	6.22	0.154	0

FIGURE CAPTIONS

- Fig. 1. Evolutionary tracks of the core helium burning stars in the HR diagram. The initial stellar mass M_{ZAMS} is indicated near each track. Parts of tracks corresponding to the instability of the star against radial oscillations are shown by dotted lines.
- Fig. 2. The kinetic energy growth rate η versus the mean effective temperature $\langle T_{\text{eff}} \rangle$ of the star evolving across the Cepheid instability strip. The dotted and dash-dotted lines correspond to the blueward and redward evolution, respectively. Each pair of plots is arbitrarily shifted along the vertical axis and the horizontal dashed line indicates $\eta = 0$. Initial stellar masses M_{ZAMS} are indicated near the plots.
- Fig. 3. The period of radial oscillations Π of the Cepheid with initial mass $M_{\text{ZAMS}} = 8M_{\odot}$ as a function of the evolution time t_{ev} counted from the moment when the star enters the instability strip. Hydrodynamical models are shown by filled circles ($\eta > 0$) and open circles ($\eta < 0$). The second-order algebraic polynomial approximation is shown in dotted (blueward evolution in the HR diagram) and dash-dotted (redward evolution) lines.
- Fig. 4. Same as Fig. 3 but for $M_{\text{ZAMS}} = 6M_{\odot}$. Plots with periods $\Pi > 6$ day and $\Pi < 6$ correspond to radial pulsations in the fundamental mode and the first overtone, respectively.
- Fig. 5. The dimensionless period change rate $\dot{\Pi}$ as a function of the pulsation period Π for Cepheids during the first crossing of the instability strip. Relations (1) are shown in dashed lines for oscillations in the fundamental mode ($\Pi > 6.9$ day) and the first overtone ($\Pi < 4.5$ day).
- Fig. 6. Same as Fig. 5 but for Cepheids during the second crossing of the instability strip.
- Fig. 7. The dimensionless period change rate $\dot{\Pi}$ versus the pulsation period Π (in days) for Cepheids during the first (a) and the second (b) crossings of the instability strip. Observational data by Pietrukowicz (2001) and Poleski (2008) are shown in filled circles and open circles, respectively. Results of theoretical computations are shown in solid lines. Initial stellar masses are indicated at the curves. The unlabelled curve corresponds to the first overtone Cepheids with $M_{\text{ZAMS}} = 6M_{\odot}$.

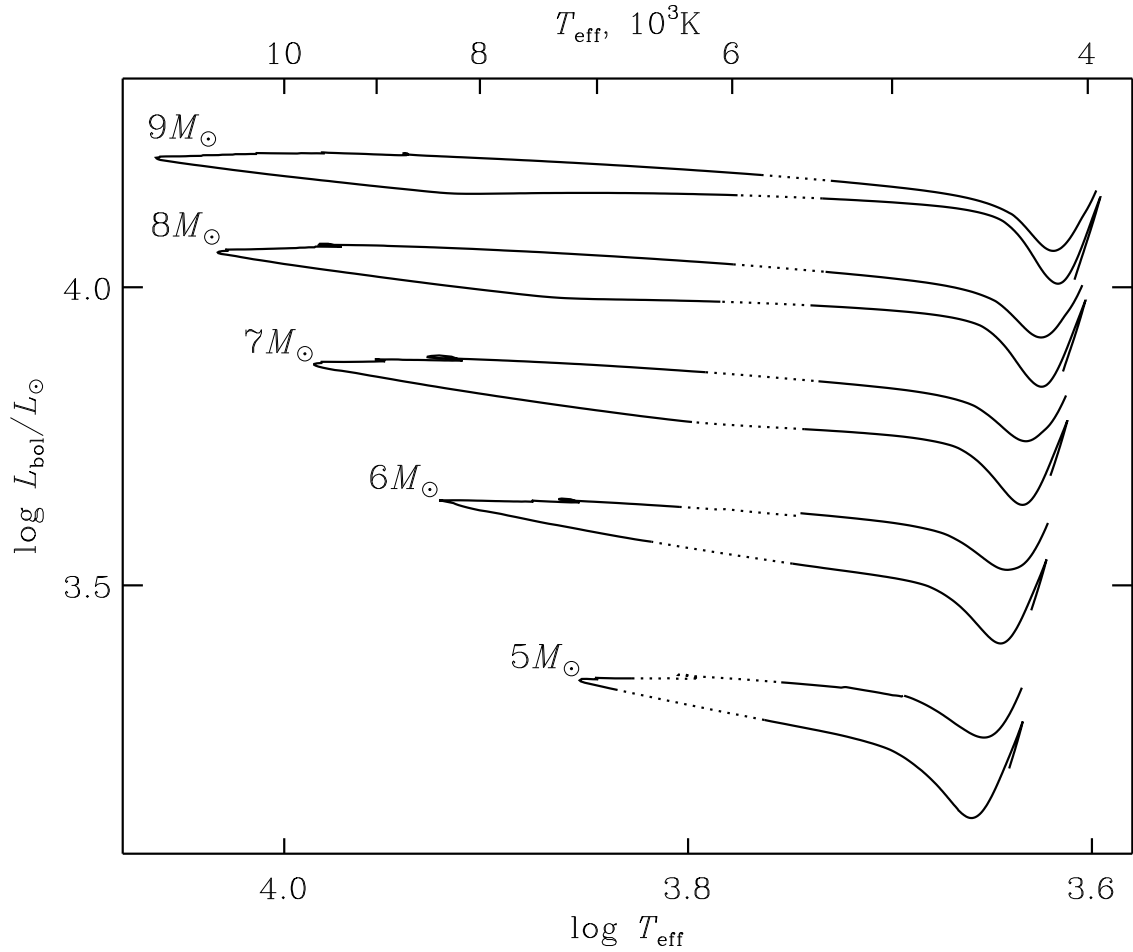


Figure 1: Evolutionary tracks of the core helium burning stars in the HR diagram. The initial stellar mass M_{ZAMS} is indicated near each track. Parts of tracks corresponding to the instability of the star against radial oscillations are shown by dotted lines.

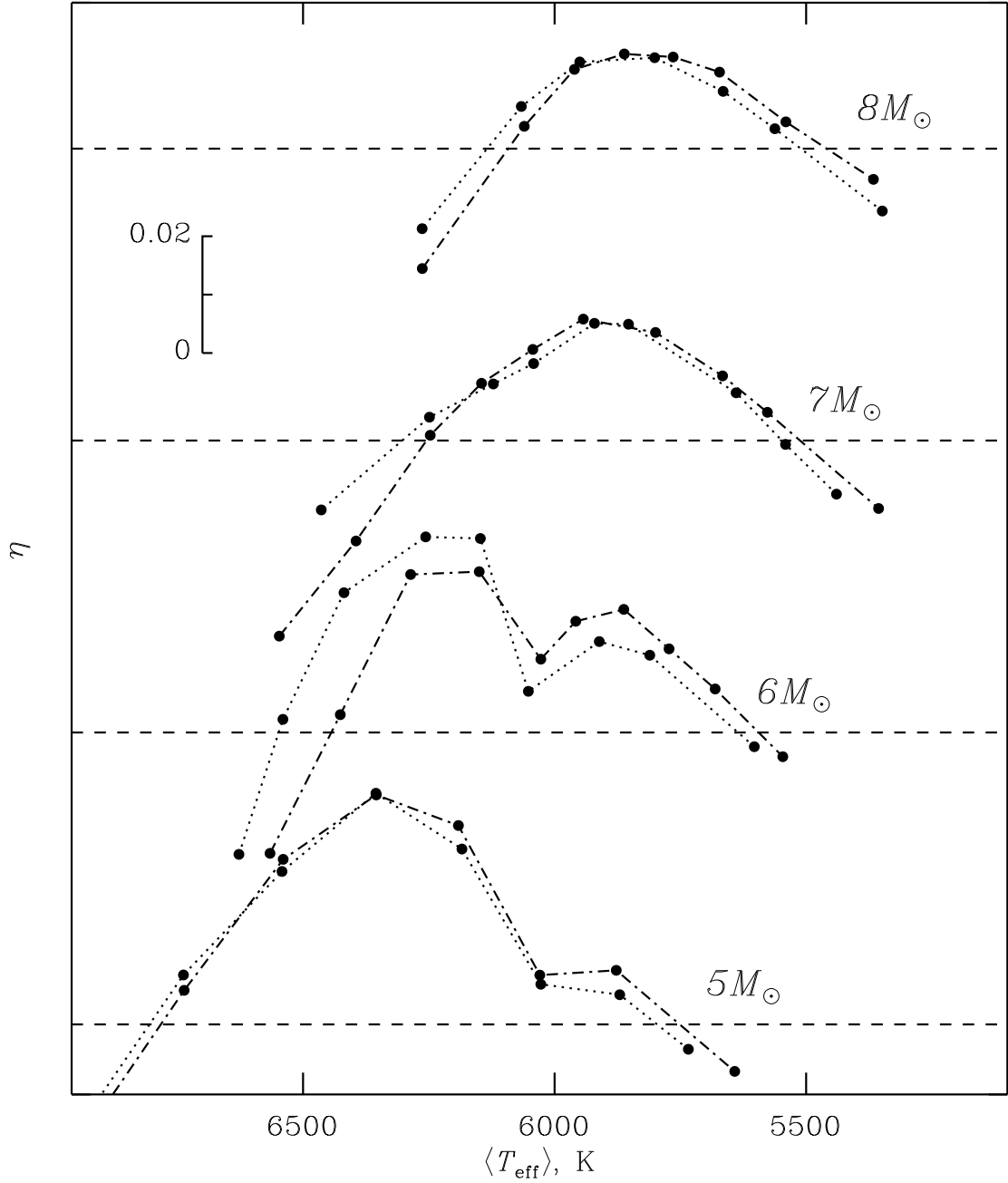


Figure 2: The kinetic energy growth rate η versus the mean effective temperature $\langle T_{\text{eff}} \rangle$ of the star evolving across the Cepheid instability strip. The dotted and dash–dotted lines correspond to the blueward and redward evolution, respectively. Each pair of plots is arbitrarily shifted along the vertical axis and the horizontal dashed line indicates $\eta = 0$. Initial stellar masses M_{ZAMS} are indicated near the plots.

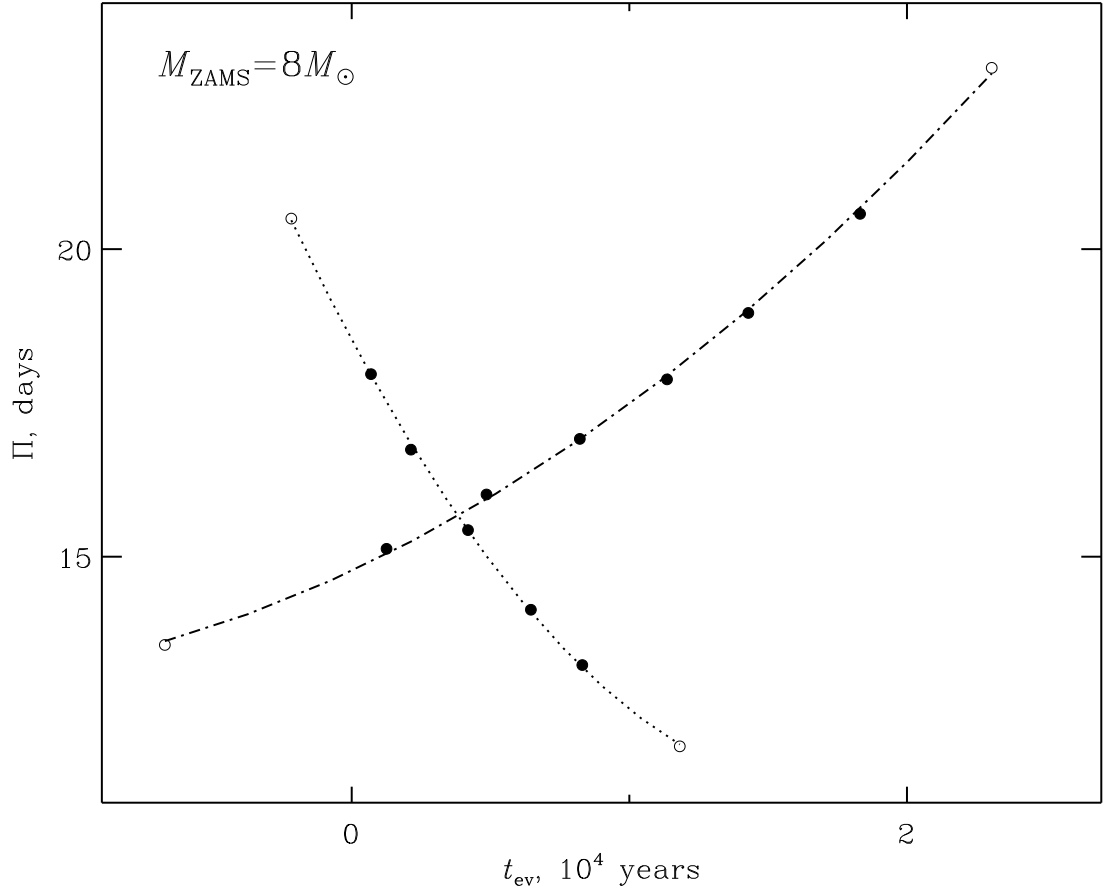


Figure 3: The period of radial oscillations Π of the Cepheid with initial mass $M_{ZAMS} = 8M_{\odot}$ as a function of the evolution time t_{ev} counted from the moment when the star enters the instability strip. Hydrodynamical models are shown by filled circles ($\eta > 0$) and open circles ($\eta < 0$). The second-order algebraic polynomial approximation is shown in dotted (blueward evolution in the HR diagram) and dash-dotted (redward evolution) lines.

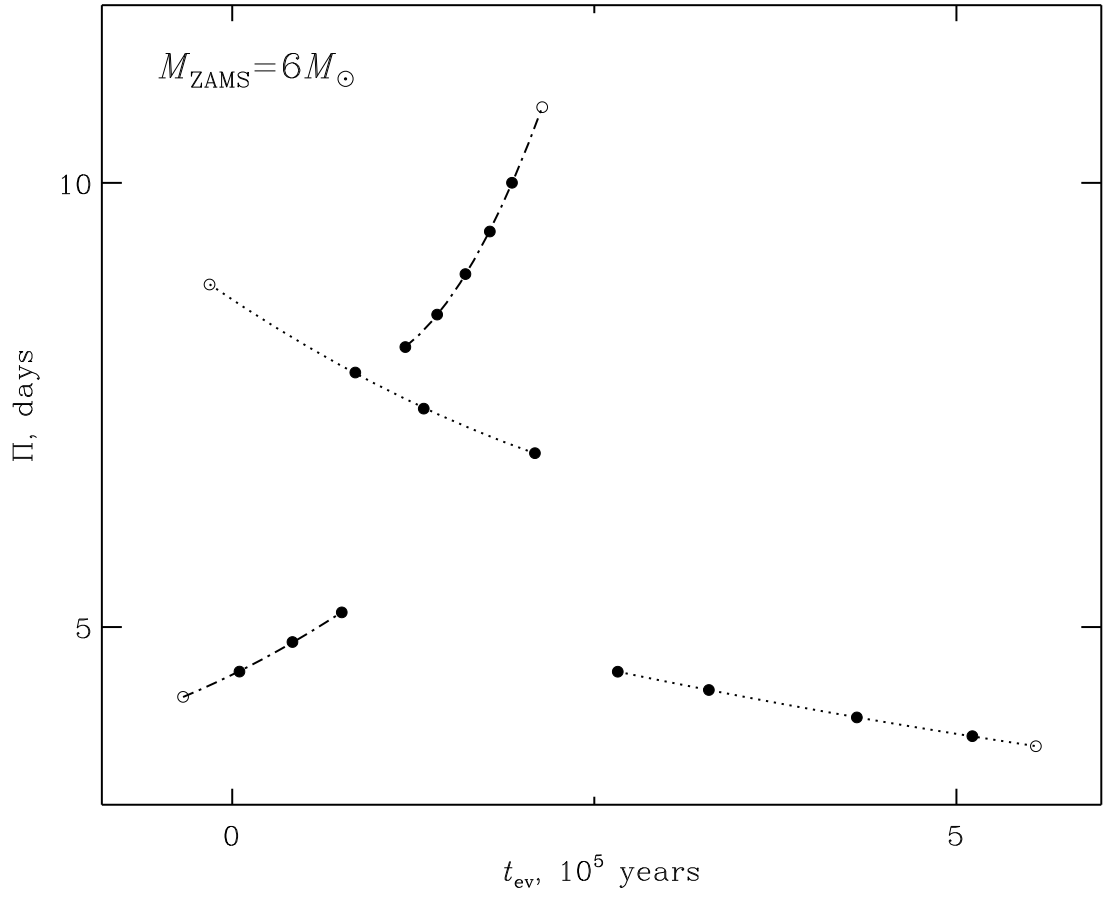


Figure 4: Same as Fig. 3 but for $M_{\text{ZAMS}} = 6M_{\odot}$. Plots with periods $\Pi > 6$ day and $\Pi < 6$ correspond to radial pulsations in the fundamental mode and the first overtone, respectively.

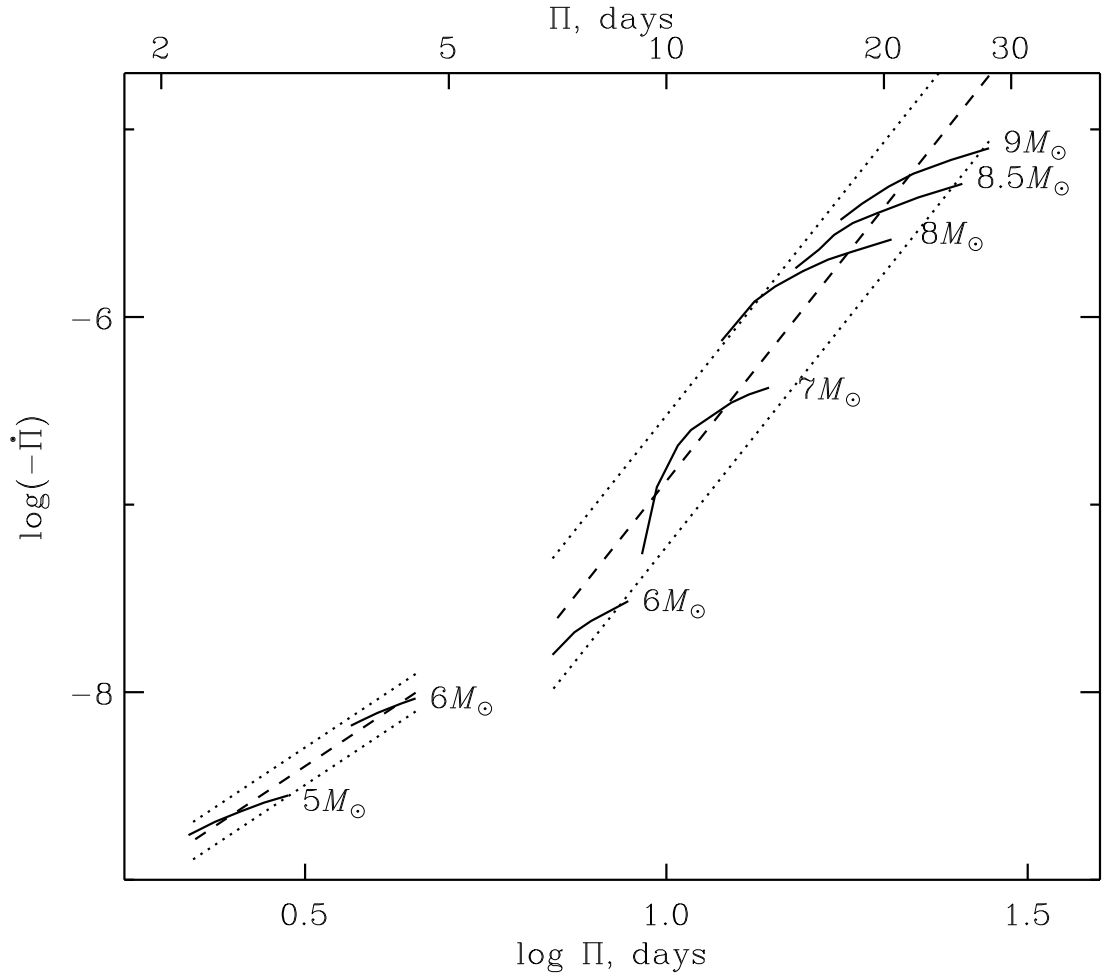


Figure 5: The dimensionless period change rate $\dot{\Pi}$ as a function of the pulsation period Π for Cepheids during the first crossing of the instability strip. Relations (1) are shown in dashed lines for oscillations in the fundamental mode ($\Pi > 6.9$ day) and the first overtone ($\Pi < 4.5$ day).

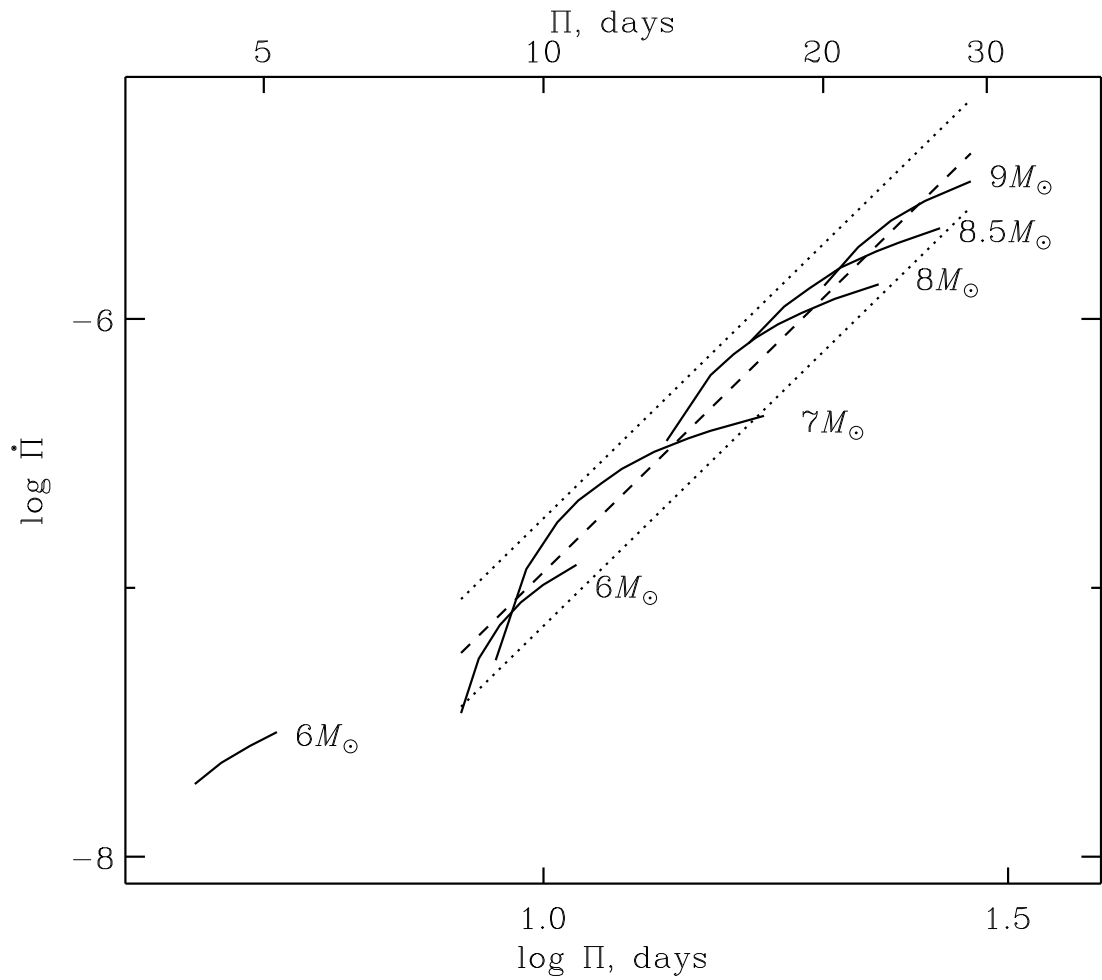


Figure 6: Same as Fig. 5 but for Cepheids at the second crossing of the instability strip.

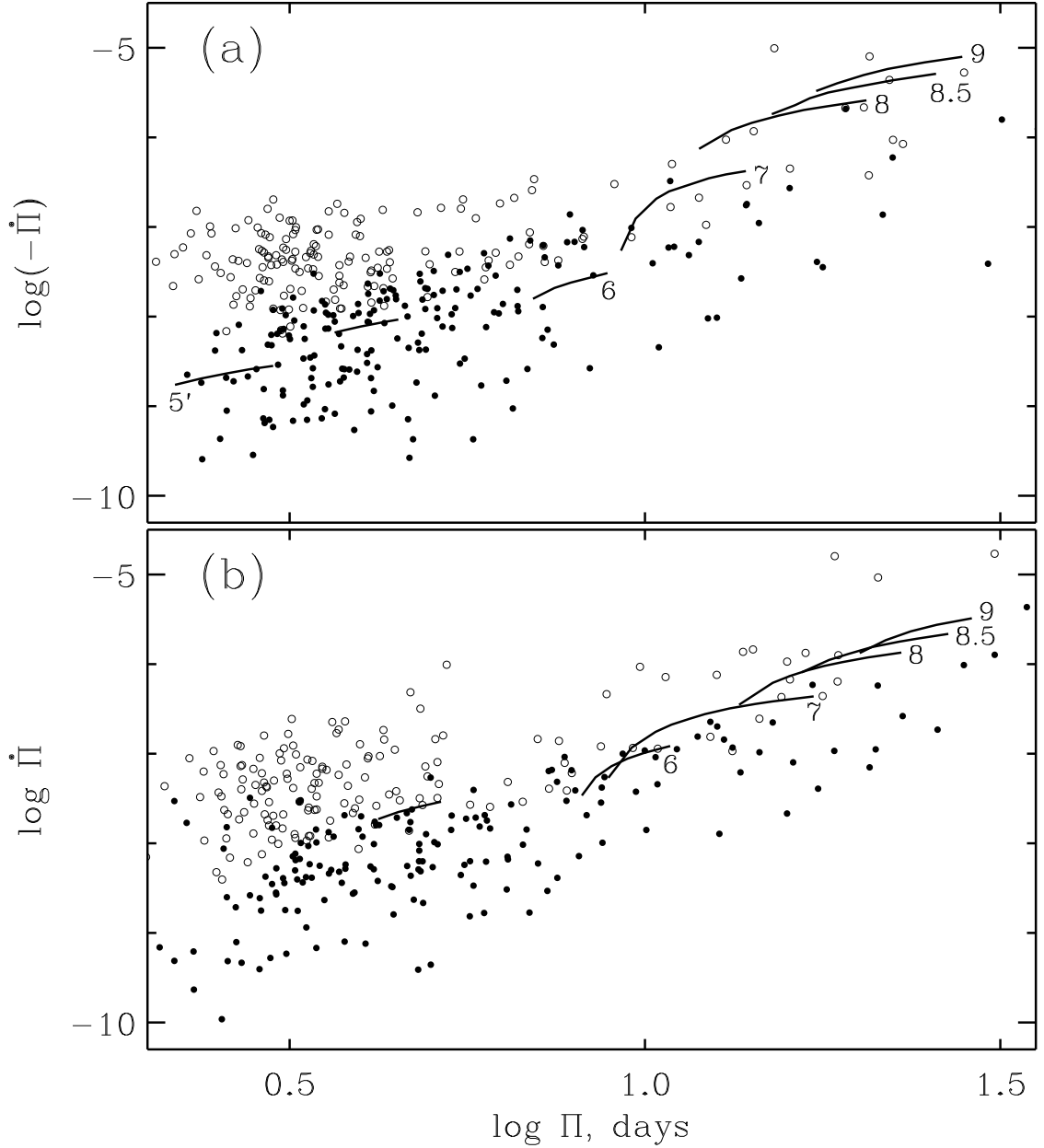


Figure 7: The dimensionless period change rate $\dot{\Pi}$ versus the pulsation period Π (in days) for Cepheids during the first (a) and the second (b) crossings of the instability strip. Observational data by Pietrukowicz (2001) and Poleski (2008) are shown in filled circles and open circles, respectively. Results of theoretical computations are shown in solid lines. Initial stellar masses are indicated at the curves. The unlabelled curve corresponds to the first overtone Cepheids with $M_{\text{ZAMS}} = 6M_{\odot}$.